The damping of a truss structure with a piezoelectric transducer

A. Preumont * , B. de Marneffe , A. Deraemaeker

ULB, Active Structures Laboratory
Av. F. Roosevelt 50 CP165/42, 1050 Brussels, Belgium

F. Bossens

Micromega Dynamics sa, rue des Chasseurs Ardennais, 4031 Liège, Belgium

Abstract

This paper re-examines the classical problem of active and passive damping of a piezoelectric truss. The active damping strategy is the so-called IFF (Integral Force Feedback) which has guaranteed stability; both voltage control and charge (current) control implementations are examined; they are compared to resistive shunting. It is shown that in all three cases, the closed-loop eigenvalues follow a root-locus; closed form analytical formulas are given for the poles and zeros and the maximum modal damping. It is shown that the performances are controlled by two parameters: the modal fraction of strain energy ν_i in the active strut and the electromechanical coupling factor k. The paper also examines the damping via inductive shunting and the enhancement of the electromechanical coupling factor by shunting a synthetic negative capacitance.

In the second part, a numerical example is examined and the analytical formulae are compared with predictions based on more elaborate models, including a full FE representation of the truss, the transducer, the electrical network and the controller. The limitations of the analytical formulae are pointed out.

Key words: Piezoelectric transducers, piezoelectric truss, active and passive damping, Integral Force Feedback, voltage control, charge control, resistive shunt, inductive shunting, negative capacitance

* Corresponding author. Tel: +32 2 650 26 89
Email address: Andre.Preumont@ulb.ac.be (A. Preumont).

1 Introduction

The active damping of a truss with piezoelectric struts has been largely motivated by producing large, lightweight spacecrafts with improved dynamic stability; this classical problem has received a lot of attention over the past 15 years and very effective solutions have been proposed (e.g.[1]). One of them known as Integral Force Feedback (IFF) is based on a collocated force sensor and has guaranteed stability [2].

Traditionally, the piezoelectric actuators have been controlled with a voltage amplifier; this is known to lead to substantial hysteresis caused by the ferroelectric behavior of the material, which requires an external sensor and closed-loop control for precision engineering applications. On the contrary, charge control allows to achieve a nearly linear relationship between the driving electrical value and the free actuator extension (e.g.[3]). The theory of IFF with charge control, and its implementation with a current amplifier, was reexamined in [4].

For space applications, because of the inherent constraints of the launch loads, the space environment, and the impossibility of in-orbit maintenance, there is a strong motivation to reduce or eliminate the power electronics associated to the piezoelectric actuators as well as the complex electronics associated to sensing (particularly in the sub-micron range where the sensor sensitivity becomes an issue). This has motivated the use of passive electrical networks as damping mechanisms [5], [6], [7]. The efficiency of such a damping mechanism depends very much on the ability to transform mechanical (strain) energy into electrical energy, that is to transfer strain from the vibrating structure to the transducer material, and to transform the strain energy into electrical energy inside the active material; the latter is measured by the *electromechanical coupling factor* k. Recent improvements have led to piezoelectric materials with coupling factors of $k_{33} = 0.7$ and more, making them a very attractive option for damping passively space structures. This paper compares the passive and the active options; they are presented in a very similar formalism and closed-loop results are presented, which allow a direct evaluation of the performances in terms of two physical parameters: the *modal fraction of strain energy* ν_i which controls the ability of every vibration mode to concentrate the strain energy into the transducer element, and the electromechanical coupling factor which measures the material ability to transform mechanical strain energy into electrical energy. Furthermore, the electromechanical coupling factor can be increased actively by shunting the piezoelectric transducer with a synthetic negative capacitance, as proposed by Forward [14] and demonstrated in [11].

Inductive shunting was first proposed in [5]; if the piezoelectric transducer is shunted on a RL circuit such that the natural frequency of the electrical

circuit is tuned on the natural frequency of one mode, the system behaves like a tuned mass damper [7]. Remarkable performances can be achieved if the shunt parameters are perfectly tuned, but they drop rapidly when the natural frequency drifts away from its design value. The extension to multiple modes is addressed in [8], where the use of a set of parallel shunts is suggested; other methods are reviewed in [9].

More recently, promising alternative methods based on state switching have been proposed. The transducer is connected to a solid-state switch device which discharges periodically the piezoelectric element on a small inductor, producing a voltage inversion [15]. Nonlinear techniques will not be addressed in this paper.

2 Governing equations

Consider the linear structure of Fig.1, assumed undamped for simplicity, and equipped with a discrete piezoelectric transducer of the stacked design (d_{33}). The stack includes n disks; its stiffness with short-circuited electrode is K_a and its unloaded capacitance is C. The structure is defined by its mass matrix M and its stiffness matrix K (excluding the transducer). The dynamics of this system can be handled with the Lagrange equations.

Using a flux linkage formulation for the electrical quantities, the Lagrangian of the system reads

$$L = T^* + W_e^* - V \tag{1}$$

where

$$T^* = \frac{1}{2}\dot{x}^T M \dot{x} \tag{2}$$

is the kinetic coenergy of the structure,

$$V = \frac{1}{2}x^T K x \tag{3}$$

is the strain energy in the structure, excluding the piezoelectric transducer, and

$$W_e^*(\dot{\lambda}) = \frac{1}{2}C(1-k^2)\dot{\lambda}^2 + nd_{33}K_a\dot{\lambda}\Delta - \frac{1}{2}K_a\Delta^2 \tag{4}$$

is the coenergy function of the piezoelectric transducer [16]. In (4), $\dot{\lambda} = V$ is the voltage at the electrodes of the transducer, $\Delta = b^T x$ is its total extension, d_{33} the piezoelectric constant and n the number of disks in the piezo stack (the free extension is $\delta = nd_{33}V$). Note that the constitutive equations of the transducer follow from

$$Q = \frac{\partial W_e^*}{\partial \dot{\lambda}} \qquad f = -\frac{\partial W_e^*}{\partial \Delta} \tag{5}$$

One finds

$$\begin{Bmatrix} Q \\ f \end{Bmatrix} = \begin{bmatrix} C(1-k^2) & nd_{33}K_a \\ -nd_{33}K_a & K_a \end{bmatrix} \begin{Bmatrix} V \\ \Delta \end{Bmatrix} \tag{6}$$

The virtual work of the non-conservative forces is

$$\delta W_{nc} = I\delta\lambda - \frac{\dot{\lambda}}{R}\delta\lambda + F\delta x \tag{7}$$

where I is the current source intensity and F is the vector of external forces applied to the structure. We assume $F = 0$ in this discussion.

The Lagrange's equations relative to the generalized coordinates x and λ give respectively

$$M\ddot{x} + (K + K_a bb^T)x = bK_a nd_{33}V \tag{8}$$

$$\frac{d}{dt}[C(1-k^2)V + nd_{33}K_a b^T x] + \frac{V}{R} = I \tag{9}$$

where $V = \dot{\lambda}$. These two equations govern the system dynamics when a current source is used. When a voltage source is used instead (the shunted resistor becomes irrelevant in this case), λ ceases to be a generalized variable and Equ.(8) applies alone.

3 Active damping with IFF and voltage control

Equation (8) is rewritten in Laplace form

$$Ms^2x + (K + K_a bb^T)x = bK_a\delta \tag{10}$$

where s is the Laplace variable and δ is the free expansion of the transducer under V. We assume that a force sensor is collocated with the piezoelectric transducer and measures the axial force f acting on the transducer. According to the second constitutive equation (6),

$$y = f = K_a(\Delta - \delta) = K_a(b^T x - \delta) \tag{11}$$

The *Integral Force Feedback (IFF)* consists of

$$\delta = \frac{g}{K_a s}y \tag{12}$$

Combining (10-12), one easily gets the closed-loop equation

$$[Ms^2 + (K + K_a bb^T) - \frac{g}{s+g}(K_a bb^T)]x = 0 \tag{13}$$

The asymptotic roots for $g \to 0$ (open-loop poles) satisfy

$$[Ms^2 + (K + K_a bb^T)]x = 0 \tag{14}$$

The solutions of this eigenvalue problem are the natural frequencies of the global structure *when the electrodes of the transducer are short-circuited*. On the other hand, the asymptotic roots for $g \to \infty$ are the open-loop zeros z_i, solutions of the eigenvalue problem

$$[Ms^2 + K]x = 0 \tag{15}$$

which corresponds to the situation where *the axial stiffness of the active strut has been removed*.

3.1 Modal coordinates

The development follows closely that of [2]. The characteristic equation is transformed in modal coordinates according to $x = \Phi z$, where $\Phi = (\phi_1, \ldots, \phi_n)$ is the matrix of the mode shapes, solutions of the eigenvalue problem (14). The mode shapes are normalized according to

$$\Phi^T M \Phi = I$$

$$\Phi^T (K + K_a bb^T)\Phi = \omega^2 = diag(\omega_i^2) \tag{16}$$

where ω_i are the natural frequencies of the structure with short-circuited electrodes. Using the modal expansion of the dynamic flexibility matrix, the open-loop Frequency Response Function (FRF) of the system can be written ([2], p.61):

$$G(\omega) = \frac{y}{\delta} = K_a[\sum_{i=1}^{n} \frac{\nu_i}{1 - \omega^2/\omega_i^2} - 1] \tag{17}$$

where the sum extends to all the modes and

$$\nu_i = \frac{\phi_i^T (K_a bb^T)\phi_i}{\phi_i^T (K + K_a bb^T)\phi_i} \tag{18}$$

is the fraction of modal strain energy in the active strut when the truss vibrates according to mode i. All the residues ν_i in the open-loop FRF are positive, which guarantees alternating poles and zeros [12], Fig.2(a). The root locus plot corresponding to the IFF is shown in Fig.3.

Transforming (13) in modal coordinates, one gets

$$[Is^2 + \omega^2 - \frac{g}{s+g}\Phi^T (K_a bb^T)\Phi]z = 0 \tag{19}$$

where the matrix $\Phi^T(K_a bb^T)\Phi$ is in general fully populated. Assuming that it is diagonally dominant, and neglecting the off-diagonal terms, it can be rewritten

$$\Phi^T(K_a bb^T)\Phi \simeq diag(\nu_i \omega_i^2) \tag{20}$$

In this case, (19) is reduced to a set of uncoupled equations:

$$s^2 + \omega_i^2 - \frac{g}{s+g}\nu_i\omega_i^2 = 0 \tag{21}$$

If one uses the notation

$$z_i^2 = \omega_i^2(1-\nu_i) \tag{22}$$

(21) can be transformed into

$$1 + g\frac{s^2+z_i^2}{s(s^2+\omega_i^2)} = 0 \tag{23}$$

which shows that every mode follows a root locus with poles at $\pm j\omega_i$ and at $s=0$, and zeros at $\pm jz_i$ (Fig.4). Comparing with (15), the latter are readily identified as the natural frequencies of the structure when the axial stiffness of the active strut has been cancelled. If $z_i \geq \omega_i/3$, the maximum modal damping is given by

$$\xi_i^{max} = \frac{\omega_i - z_i}{2z_i} \tag{24}$$

and is achieved for $g = \omega_i\sqrt{\omega_i/z_i}$ [2]. If $z_i < \omega_i/3$, $\xi_i > 1$, see Fig.11.

Note that, since (22) is approximate, one can use the roots of (15) as z_i when drawing the root locus (23).

4 Active Damping with IFF and charge control

If one considers a pure current source, $R \to \infty$ in (9). Upon eliminating V between (8) and (9), it is easily established that the dynamics of the system is now governed by

$$M\ddot{x} + [K + bb^T\frac{K_a}{1-k^2}]x = b\frac{K_a}{1-k^2}.d_{33}n\frac{I}{sC} \tag{25}$$

where

$$k^2 = \frac{d_{33}^2}{s^E\varepsilon^T} = \frac{n^2d_{33}^2K_a}{C} \tag{26}$$

k is the electromechanical coupling factor of the transducer material. I/s is the electric charge Q and $\delta = nd_{33}Q/C$ is the free expansion of the transducer under Q (and $f=0$). Equation (25) is very similar to (10), except that the piezoelectric transducer behaves with an increased stiffness, $K_a/(1-k^2)$, corresponding to open electrodes ($Q=0$).

Using the same force feedback as in section 3 (IFF on Q, which amounts to proportional feedback on I), after modifying slightly (11) and (12) to account for the increased stiffness of the transducer, one easily gets that the closed-loop poles are solution of the eigenvalue problem

$$[Ms^2 + (K + \frac{K_a}{1-k^2}bb^T) - \frac{g}{s+g}\frac{K_a}{1-k^2}bb^T]x = 0 \tag{27}$$

The asymptotic roots for $g = 0$ satisfy

$$[Ms^2 + (K + \frac{K_a}{1-k^2}bb^T)]x = 0 \tag{28}$$

The solutions are the natural frequencies of the global structure, Ω_i, *when the transducer electrodes are open*. On the other hand, the asymptotic roots when $g \to \infty$, which are the open-loop zeros, z_i, are again solutions of the eigenvalue problem (15).

Following the same procedure as in the previous section, (27) can be transformed into modal coordinates; it is readily found that the closed-loop poles are solutions of

$$1 + g\frac{s^2 + z_i^2}{s(s^2 + \Omega_i^2)} = 0 \tag{29}$$

which is the same as (23), except that the natural frequencies Ω_i with open electrodes are used instead of ω_i (with short-circuited electrodes). The root locus is again that of Fig.4, and the maximum damping ratio is given by (24) with Ω_i instead of ω_i. Note that, assuming that the displacement mode shapes are independent of the electric boundary conditions,

$$\Omega_i^2 = \phi_i^T(K + \frac{K_a}{1-k^2}bb^T)\phi_i = \phi_i^T(K + K_a bb^T)\phi_i + \frac{k^2}{1-k^2}\phi_i^T K_a bb^T \phi_i$$

or, using (16) and (18),

$$\Omega_i^2 \simeq \omega_i^2(1 + \frac{k^2}{1-k^2}\nu_i) \tag{30}$$

5 Admittance of the transducer

The admittance of the transducer installed in the structure can be analyzed with (8) and (9), after removing the resistive shunting ($R \to \infty$). Upon eliminating x between the two equations, one can show that (see [16] p.117 for details)

$$\frac{I}{sCV} = 1 + k^2[\sum_{i=1}^{n}\frac{\nu_i}{1 - \omega^2/\omega_i^2} - 1] \tag{31}$$

which is quite similar to (17). It is represented in Fig.2(b); it also exhibits alternating poles and zeros. The poles are at ω_i, the natural frequencies of the structure with short-circuited electrodes, and it can be shown that the zeros are at Ω_i, the natural frequencies with open electrodes ($I = 0$). The interesting thing is that a single admittance test allows to determine both ω_i and Ω_i.

6 Passive damping via resistive shunting

Setting $I = 0$ in (9) and eliminating V between (8) and (9), one gets the eigenvalue problem

$$[Ms^2 + (K + K_a bb^T) + \frac{k^2 K_a bb^T}{(1-k^2) + 1/sRC}]x = 0 \tag{32}$$

One sees that when $R = 0$, it is identical to (14), leading to the frequencies ω_i (short-circuited). For $R \to \infty$, it becomes identical to (28), leading to Ω_i (open electrodes). Going into modal coordinates, denoting $\varrho = RC$, one finds that every mode follows the characteristic equation

$$s^2 + \omega_i^2 + \frac{k^2 \nu_i \omega_i^2}{1 - k^2 + 1/\varrho s} = 0 \tag{33}$$

which can be rewritten in a root locus form

$$1 + \frac{1}{\varrho(1-k^2)} \frac{s^2 + \omega_i^2}{s(s^2 + \Omega_i^2)} = 0 \tag{34}$$

where (30) has been used. According to this equation, when ϱ varies from ∞ to 0, the poles follow a root locus similar to that of Fig.4. The poles are in this case at $\pm j\Omega_i$ (open electrodes) while the zeros are at $\pm j\omega_i$ (short-circuited). As in Fig.4, the maximum achievable damping is given by

$$\xi_i^{max} = \frac{\Omega_i - \omega_i}{2\ \omega_i} \simeq \frac{\Omega_i^2 - \omega_i^2}{4\ \omega_i^2} \tag{35}$$

and, using again (30),

$$\xi_i^{max} = \frac{k^2 \nu_i}{4(1-k^2)} \tag{36}$$

(it is achieved for $[\rho(1-k^2)]^{-1} = \Omega_i \sqrt{\Omega_i/\omega_i}$.) This equation points out the influence of the fraction of modal strain energy ν_i and the electromechanical coupling factor on passive damping with resistive shunting. Note that all the modes cannot be optimally damped simultaneously, because there is a single tuning parameter ϱ.

Figure 5 and Table 1 summarize the results of the three control configurations. Column 4 of Table 1 gives an approximation of the maximum achievable modal damping based on (35); these expressions show clearly the influence of the fraction of modal strain energy ν_i and that of the electromechanical coupling factor k. Note that: *(i)* For the IFF with voltage control, the maximum damping is independent of the electromechanical coupling factor. *(ii)* The IFF with charge control gives always better performances than with voltage control; the advantage increases with k. *(iii)* Significant modal damping with resistive shunting can be achieved only when the electromechanical coupling factor is large; piezoelectric materials with $k \geq 0.7$ are available.

7 Generalized electromechanical coupling factor

It is well known that the electromechanical coupling factor of a piezoelectric transducer alone can be derived from an admittance measurement. If p and z are respectively the pole and the zero in the admittance curve,

$$k^2 = \frac{z^2 - p^2}{z^2} \tag{37}$$

By analogy, if we consider the poles ω_i and zeros Ω_i in the admittance curve of the transducer when it is mounted in the structure, one can define the generalized electromechanical coupling factor of mode i as

$$K_i^2 = \frac{\Omega_i^2 - \omega_i^2}{\Omega_i^2} \tag{38}$$

Using (30), one finds

$$K_i^2 = \frac{k^2 \nu_i}{1 - k^2 + k^2 \nu_i} \tag{39}$$

K_i^2 combines material data with information about the structure; $K_i^2 = k^2$ if $\nu_i = 1$. Note that, in the literature, the definition

$$K_i^2 = \frac{\Omega_i^2 - \omega_i^2}{\omega_i^2} = \frac{k^2 \nu_i}{1 - k^2} \tag{40}$$

is often used instead of (38). The difference between the two definitions is insignificant in most practical applications, but (40) does not supply $K_i = k$ if $\nu_i = 1$. The maximum performance of resistive shunting, (36), is directly related to the generalized electromechanical coupling factor.

8 Damping enhancement via negative capacitive shunting

Equation (36) indicates that the damping performance of the resistive shunting depends critically on the electromechanical coupling factor, and that it may become significant if $k > 0.7$. The electromechanical coupling factor of the transducer can be increased by placing a negative capacitance in parallel to the transducer (Fig.6).

The properties $(C^\star, k^\star)$ of the equivalent transducer can be determined by equating the joint coenergy function of the original transducer and the negative capacitance $-C_1$

$$W_e^*(\dot{\lambda}) = \frac{1}{2}C(1-k^2)\dot{\lambda}^2 + nd_{33}K_a\dot{\lambda}\Delta - \frac{1}{2}K_a\Delta^2 - \frac{1}{2}C_1\dot{\lambda}^2 \tag{41}$$

with the coenergy function of the equivalent transducer

$$W_e^*(\dot{\lambda}) = \frac{1}{2}C^*(1-k^{*2})\dot{\lambda}^2 + nd_{33}K_a\dot{\lambda}\Delta - \frac{1}{2}K_a\Delta^2 \tag{42}$$

One finds easily that the equivalent properties are

$$C^* = C - C_1 \tag{43}$$

$$k^{*2} = k^2\frac{C}{C-C_1} \tag{44}$$

Note that, since $k^{\star 2} < 1$, one must have $C_1 < C(1-k^2)$.

Returning to (30) and Fig.5, one sees that a negative capacitance increases the natural frequency with open electrodes, Ω_i, and widens the loop of the root locus for resistive shunting.

The idea of using a negative capacitance to enhance the damping was first proposed by Forward [14]; this idea is also developed in [11]. The synthesis of a negative capacitance is discussed in [13].

9 Passive damping via inductive shunting

The principle of inductive shunting is well known; the shunt consists of an inductor and a resistor in series which are combined with the capacitance of the transducer to create a damped electric resonance; if the electrical resonance is tuned on the mechanical resonance, the resonant shunt acts as a vibration absorber. The theory of inductive shunting was first presented by Hagood and von Flotow [6]; it is not easy to present it in a simple way.

Consider the system of Fig.7. In this case, it is simpler to use the electric charge as electric variable in the formulation of the Lagrange equations (rather than the flux linkage used earlier in this paper). Let $\dot{q}$ be the current in the single electrical loop of the system; the Lagrangian reads in this case

$$L = T^\star + W_m^\star - V - W_e \tag{45}$$

where $T^\star$ and V refer, as usual, to the mechanical part of the system, $W_m^\star = (1/2)L\dot{q}^2$ is the magnetic coenergy of the inductor and W_e is the electromechanical energy of the piezoelectric transducer,

$$L = \frac{1}{2}\dot{x}^T M\dot{x} + \frac{1}{2}L\dot{q}^2 - \frac{1}{2}x^T Kx - \frac{q^2}{2C(1-k^2)} + \frac{nd_{33}K_a}{C(1-k^2)}qb^T x - \frac{K_a}{1-k^2}\frac{(b^T x)^2}{2} \tag{46}$$

The Lagrange equation relative to the coordinates x and q are respectively

$$M\ddot{x} + (K + \frac{K_a}{1-k^2}bb^T)x - \frac{bnd_{33}K_a}{C(1-k^2)}q = 0 \tag{47}$$

$$L\ddot{q} + R\dot{q} + \frac{q}{C(1-k^2)} - \frac{nd_{33}K_a}{C(1-k^2)}b^T x = 0 \tag{48}$$

The electrical frequency and the electrical damping are defined respectively by

$$\omega_e^2 = \frac{1}{LC(1-k^2)} \tag{49}$$

$$2\xi_e\omega_e = \frac{R}{L} \tag{50}$$

With these notations, (48) is rewritten (in Laplace form)

$$q = \frac{\omega_e^2}{s^2 + 2\xi_e\omega_e s + \omega_e^2} nd_{33}K_a b^T x \tag{51}$$

Substituting into (47), one finds

$$(Ms^2 + K + \frac{K_a}{1-k^2}bb^T)x + \frac{k^2}{1-k^2}K_a bb^T x[\frac{-\omega_e^2}{s^2 + 2\xi_e\omega_e s + \omega_e^2}] = 0 \tag{52}$$

and, after transformations into modal coordinates, one finds that every mode is governed by the characteristic equation

$$s^2 + \Omega_i^2 + \frac{k^2\nu_i\omega_i^2}{1-k^2}[\frac{-\omega_e^2}{s^2 + 2\xi_e\omega_e s + \omega_e^2}] = 0 \tag{53}$$

This equation can be rearranged into a root locus form

$$1 + 2\xi_e\omega_e \frac{s(s^2 + \Omega_i^2)}{s^4 + (\Omega_i^2 + \omega_e^2)s^2 + \omega_i^2\omega_e^2} = 0 \tag{54}$$

In this formulation, $2\xi_e\omega_e$ plays the role of the gain in a classical root locus. Note that, for large R, the poles tend to $\pm j\Omega_i$, as expected. For $R = 0$ (i.e. $\xi_e = 0$), they are the solutions p_1 and p_2 of the characteristic equation $s^4 + (\Omega_i^2+\omega_e^2)s^2+\omega_i^2\omega_e^2 = 0$ which accounts for the classical double peak of resonant dampers, with p_1 above $j\Omega_i$ and p_2 below $j\Omega_i$. Fig.8 shows the root locus for a fixed value of ω_i/Ω_i and various values of the electrical tuning, expressed by the ratio

$$\alpha_e = \frac{\omega_e\omega_i}{\Omega_i^2} \tag{55}$$

The locus consists of two loops, starting respectively from p_1 and p_2; one of them goes to $j\Omega_i$ and the other goes to the real axis, near $-\Omega_i$. If $\alpha_e > 1$ [Fig.8(a)], the upper loop starting from p_1 goes to the real axis, and that starting from p_2 goes to $j\Omega_i$, and the upper pole is always more heavily damped than the lower one (note that, if $\omega_e \to \infty$, $p_1 \to \infty$ and $p_2 \to j\omega_i$; the lower branch of the root locus becomes that of the resistive shunting). The opposite situation occurs if $\alpha_e < 1$ [Fig.8(b)]: the upper loop goes from p_1 to $j\Omega_i$ and the lower one goes from p_2 to the real axis; the lower pole is always more heavily damped. If $\alpha_e = 1$ [Fig.8(c)], the two poles are always equally damped until the two branches touch each other in Q. This double root is achieved for

$$\alpha_e = \frac{\omega_e\omega_i}{\Omega_i^2} = 1 \qquad , \qquad \xi_e^2 = 1 - \frac{\omega_i^2}{\Omega_i^2} \tag{56}$$

This can be regarded as the optimum tuning of the inductive shunting (note that, comparing with (38), $\xi_e^2 = K_i^2$; thus, the optimum electrical damping ratio exactly matches the generalized electromechanical coupling factor). The corresponding eigenvalues satisfy

$$s^2 + \Omega_i^2 + \Omega_i(\frac{\Omega_i^2}{\omega_i^2} - 1)^{1/2}s = 0 \tag{57}$$

For various values of ω_i/Ω_i (or K_i), the optimum poles at Q move along a circle of radius Ω_i [Fig.8(d)]. The corresponding damping ratio can be obtained easily by identifying the previous equation with the classical form of the damped oscillator, $s^2 + 2\xi_i\Omega_i s + \Omega_i^2 = 0$, leading to

$$\xi_i = \frac{1}{2}(\frac{\Omega_i^2}{\omega_i^2} - 1)^{1/2} = \frac{1}{2}(\frac{K_i^2}{1 - K_i^2})^{1/2} \simeq \frac{K_i}{2} \tag{58}$$

Using (30), we can express the optimum damping ratio in terms of the electromechanical coupling factor and the fraction of modal strain energy:

$$\xi_i = \frac{1}{2}(\frac{k^2\nu_i}{1 - k^2})^{1/2} \tag{59}$$

This value is significantly higher than that achieved with purely resistive shunting [it is exactly the square-root of (36)]; it has been added to Table 1

for comparison. Note, however, that it is much more sensitive to the tuning of the electrical parameters on the targeted modes. This is illustrated in Fig.9, which displays the evolution of the damping ratio ξ_i when the actual natural frequency ω_i' moves away from the nominal frequency ω_i for which the shunt has been optimized (the damping ratio associated with p_1 and p_2 is plotted in dotted lines; the ratio ω_i'/Ω_i' is kept constant in all cases). One sees that the performance of the inductive shunting drops rapidly below that of the resistive shunting when the de-tuning increases. Note that, for low frequency modes, the optimum inductance value can be very large; such large inductors can be synthesized electronically. The multimodal passive damping via resonant shunt has been investigated by Hollkamp [8].

10 Numerical example

In this section, we illustrate the foregoing theory and we point out the limitations of the analytical formulae.

Consider the truss structure of Fig.10. It consists of 12 bays of 140 mm each, made of steel bars of 4 mm diameter connected with plastic joints; it is clamped at the bottom. It is equipped with two active struts as indicated in the figure. This truss was already considered in the experimental set up of [1], but in this study, a new type of active strut is used, build from a stacked actuator (PI P-010-30H) prestressed in compression with an internal wire ($K_a = 30N/\mu m$, $C = 135nF$ and $k = 0.6$) and a force sensor. The truss model consists of beam elements, except for the piezoelectric actuator which, for convenience, is obtained by Guyan's reduction of a separate model with piezoelectric volume elements. After reduction, the transducer model has only 12 mechanical variables (6 d.o.f. at its end points) and 1 electrical variable (voltage). The structural damping is assumed $\xi = 0.1\%$.

The natural frequencies with short-circuited electrodes, ω_i, and the fraction of modal strain energy, ν_i, predicted with the nominal model are given in Table 2.

In this study, we analyze the active and passive damping of modes 1 and 2, using successively the two piezoelectric struts (one at a time, but not simultaneously). The results are predicted in three different ways:

- (**1**) Using the **approximate formulae** of Table 1, formula (39) in the text and the numerical values of Table 2.
- (**2**) Using a **specific FE model** (SAMCEF) to evaluate Ω_i and z_i, by changing the electrical boundary conditions to evaluate Ω_i, or removing the axial stiffness of the actuator to evaluate z_i. Formulae (24), (35) and (58) are used to evaluate the damping.

- (**3**) Using a **full MATLAB model** which couples the FE model, the electrical network, including the non-diagonal terms in (19), and the control law. The comparison with (**2**) gives an idea of the influence of the modal coupling.

Table 3 shows the values of Ω_i, K_i and z_i, when either strut 1 or strut 2 is active. The values reported in column (**1**) have been obtained with formulae (22), (30) and (39), while those in column (**2**) have been obtained by changing the FE model. In the latter case, the values of Ω_i and K_i exactly match those obtained from an impedance or admittance curve. Notice the very large error on the approximate formulae for z_i, due to the violation of the assumptions used in deriving (22), especially the fact that the mode shapes are drastically different after removing the axial stiffness of the strut. Formula (22) must be used with caution.

Table 4 gives the maximum modal damping ξ_i predicted for the two active struts and three control strategies: IFF with voltage control, IFF with charge control, resistive shunting. Column (**1**) is based on the approximate formulae of Table 1, column (**2**) is based on the FE prediction of the poles and zeros and formulae (24) and (35), and column (**3**) is obtained with the full model. "critical" means that $\xi_i > 1$. The explanation for these very large damping values is as follows: because of the particular design of the truss, removing the axial stiffness of the actuator almost produces a mechanism, which corresponds to one zero pair being very close to the origin. With this location of the zeros, the root locus departs significantly from the shape of Fig.4. Figure 11 illustrates how the root locus of the IFF evolves when the open loop zeros migrate towards the origin.

Figure 12 shows the root locus of the closed-loop poles of the IFF with voltage control, charge control, and resistive shunting. For strut 1, Fig.12(a), the curves relative to mode 1 differ significantly from Fig.4, for the reason mentioned before; those relative to mode 2 can hardly be seen, because mode 2 is almost uncontrollable from strut 1 (ν_2 close to 0). The vicinity of ω_1 and ω_2 has been enlarged. Note that the natural frequencies with open electrodes, Ω_1 is very close to ω_1, in spite of the reasonable value of ν_1 and the electromechanical coupling factor ($k = 0.6$); this is translated into a modest value of the damping ratio achievable with resistive shunting. Examining the root locus for strut 2, Fig.11(b), one sees that, due to the weak controllability of mode 1 from strut 2, there is a permutation in the zeros z_1 and z_2: the pole at ω_2 goes to the low frequency zero while the loop of mode 1 moves towards the zero z_1 with a slightly *higher* frequency. Figure 13 shows the predicted admittance FRF of strut 1 and 2, obtained with the full MATLAB model; such curves contain information about ω_i, Ω_i, and K_i. Figure 13 essentially confirms the results of Fig.12, in particular that mode 2 is not controllable from strut 1.

Table 5 considers the inductive shunting. Columns (**1**) and (**2**) are based on (56) and the values of ω_i and Ω_i from Tables 2 and 3. Column (**3**) corresponds to the optimum condition Q in Fig.8. Figure 14 shows a detail of the root locus in the vicinity of mode 1 for perfect tuning of the electrical circuit (i.e. that providing equal damping to the two modes). Figure 15 shows a FRF between a lateral force applied along the truss (as indicated in Fig.10) and the velocity at the top. Fig.15(a) considers the inductive shunting with optimal frequency tuning and shows the evolution of the FRF with the electrical damping ξ_e. Figure 15(b) compares the resistive shunting and the inductive shunting (both at optimum value).

11 Conclusions

The first part of this paper reexamines the classical problem of active and passive damping of a piezoelectric truss. The active damping uses an Integral Force Feedback based on a collocated force sensor. Both voltage control and charge (current) control are considered. The passive damping considers both resistive and inductive shunting. The enhancement of the electromechanical coupling factor via a synthetic negative capacitance is also examined. The distinctive features of our contribution are:
(i) The system dynamics is formulated with the Lagrange equations, which provides fairly compact results (especially for inductive shunting)
(ii) All the strategies are presented in a unified way, using a root locus approach
(iii) Approximate analytical results are expressed in terms of two meaningful design parameters: the electromechanical coupling factor k^2 and the fraction of modal strain energy ν_i.

In the second part of the paper, a numerical example is considered. Two locations are considered for the active strut, and the various control strategies are compared. It is observed that:
(i) The active control by IFF is very effective and is able, at least in theory, to achieve critical damping.
(ii) The map of fraction of modal strain energy constitutes an excellent guide for actuator location, but the approximate analytical results, which are based on the assumption that the mode shapes are unchanged, grossly underestimate the control performance of the IFF. Especially formula (22) should be used with caution. In all circumstances, accurate performance evaluation can be obtained from (24), (35) and (58) provided separate modal analyses are conducted with appropriate boundary conditions to estimate the poles and the zeros. The influence of modal coupling is only marginal.
(iii) As long as the mode shapes do not change significantly and that the poles and zeros are not too far apart, the approximate analytical formulae based on

k and ν_i are fairly accurate and can be used for prediction purposes. This applies to resistive and inductive shunting.

12 ACKNOWLEDGMENT

This study was supported by the Inter University Attraction Pole IUAP 5 on Advanced Mechatronics Systems, and by ESA in the framework of the project *SSPA: Smart Structures for Payload and Antenna.*

References

[1] Preumont,A., J.P.Dufour, C.Malekian, Active damping by a local force feedback with piezoelectric actuators, *AIAA J. of Guidance*, vol.15, No 2, 390-395, March-April, 1992.

[2] Preumont,A. *Vibration Control of Active Structures, An Introduction*, (2nd Edition), Kluwer, 2002.

[3] Dörlemann,C., P.Muss, M.Schugt, R.Uhlenbrock, New high speed current controlled amplifier for PZT multilayer stack actuators, *ACTUATOR-2002*, Bremen, June, 2002.

[4] Preumont,A., On the damping of a piezoelectric truss, *ICTAM'04*, Warsaw, August, 2004.

[5] Forward,R.L., Electronic damping of vibrations in optical structures, *Journal of Applied Optics*, **18**, 690-697, March, 1979.

[6] Hagood,N.W., A.von Flotow, Damping of structural vibrations with piezoelectric materials and passive electrical networks, *Journal of Sound and Vibration* **146**(2), 243-268, 1991.

[7] Hagood,N.W., E.F.Crawley, Experimental investigation of passive enhancement of damping for space structures, *AIAA J. of Guidance*, vol.14, No 6, 1100-1109, Nov.Dec. 1991.

[8] Hollkamp,J.J., Multimodal passive vibration suppression with piezoelectric materials and resonant shunts, *J. Intell. Material Syst. Structures*, Vol.5, Jan.1994.

[9] Moheimani,S.O.R., A survey of recent innovations in vibration damping and control using shunted piezoelectric transducers, *IEEE Transactions on Control Systems Technology*, Vol.11, No 4, 482-494, July 2003.

[10] Edberg,D.L., A.S.Bicos, J.S.Fechter, On piezoelectric energy conversionfor electronic passive damping enhancement, Proceedings of *Damping'91*, San Diego, 1991.

[11] Park,C.H., A.Baz, Vibration control of beams with negative capacitive shunting of interdigital electrode piezoceramics, *Journal of Vibration and Control*, Vol.11: 331-346, 2005.

[12] Martin,G.D. *On the control of flexible mechanical systems*, PhD Thesis, Stanford University, 1978.

[13] Philbrick Researches, Inc., *Application Manual for Computing Amplifiers for Modelling, Measuring, Manipulating & Much Else* Nimrod Press, Boston, 1965.

[14] Forward R.L., US Patent 4,158,787, June 1979

[15] Guyomar, D., Richard, C., Non-linear and hysteretic processing of piezoelement: Application to vibration control, wave control and energy harvesting, *Int. Journal of Applied Electromagnetics and Mechanics*, 21, 193-207, 2005.

[16] Preumont, A., *Mechatronics: Dynamics of Electromechanical and Piezoelectric Systems*. Springer 2006

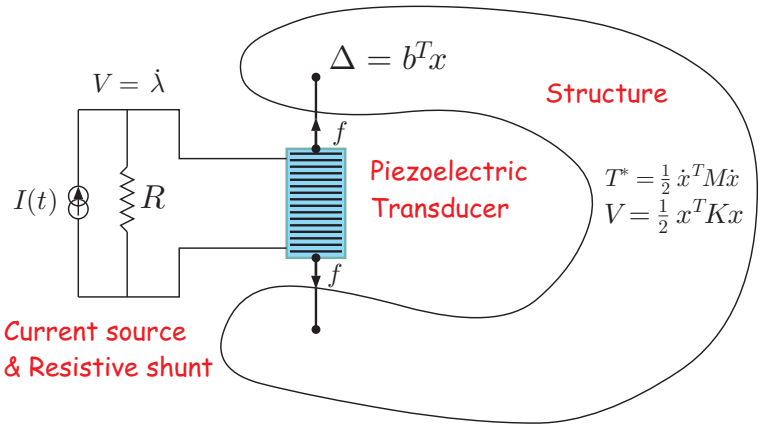

Fig. 1. Linear structure equipped with a piezoelectric transducer, a current source and a shunted resistor.

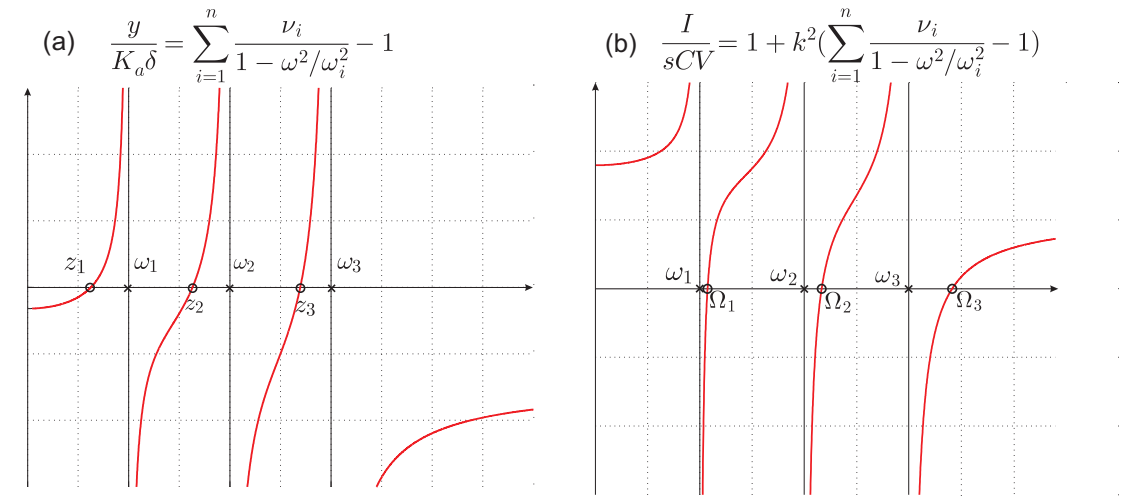

Fig. 2. (a) Open loop FRF of the active strut mounted in the structure. (b) Admittance of the transducer mounted in the structure

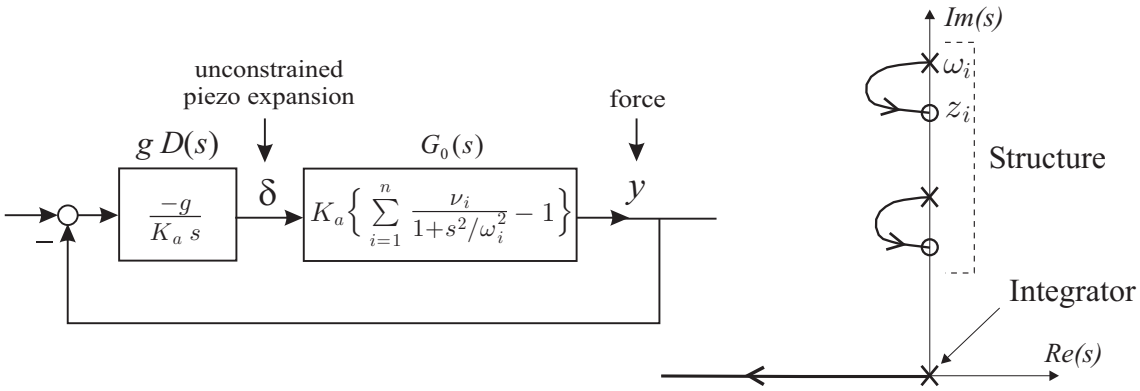

Fig. 3. (a) Block diagram of the IFF. (b) Typical root locus.

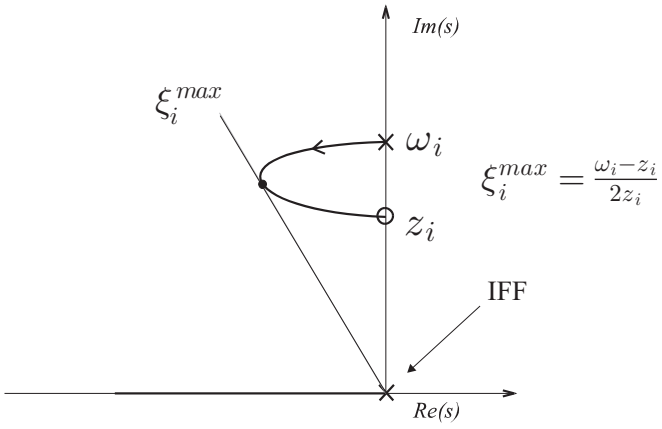

Fig. 4. Root locus of the IFF, voltage control (only half of the locus is shown).

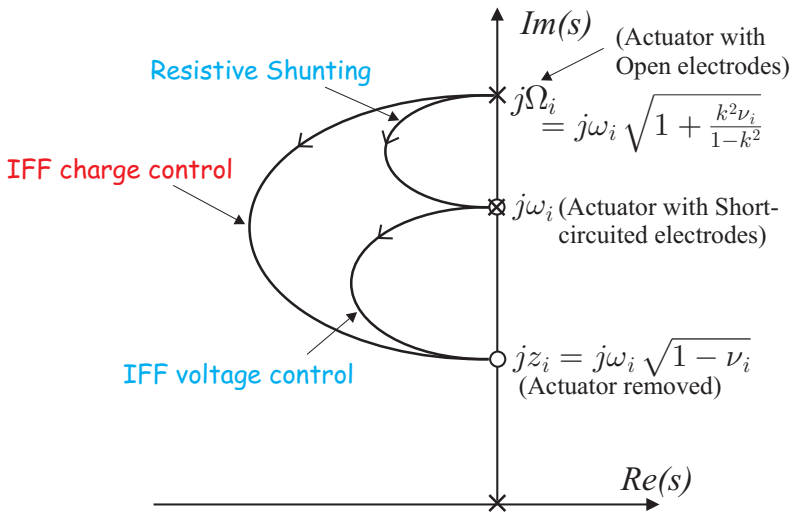

Fig. 5. Root locus plots corresponding to various control configurations.

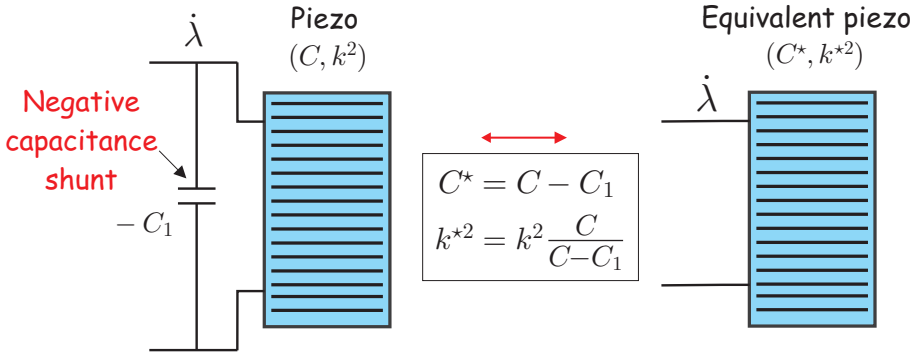

Fig. 6. Piezoelectric transducer shunted on a negative capacitance $-C_1$ and equivalent properties.

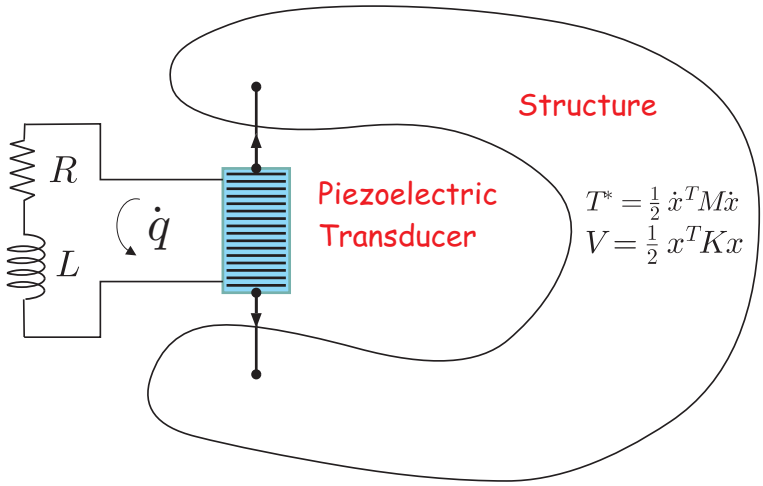

Fig. 7. Inductive shunting.

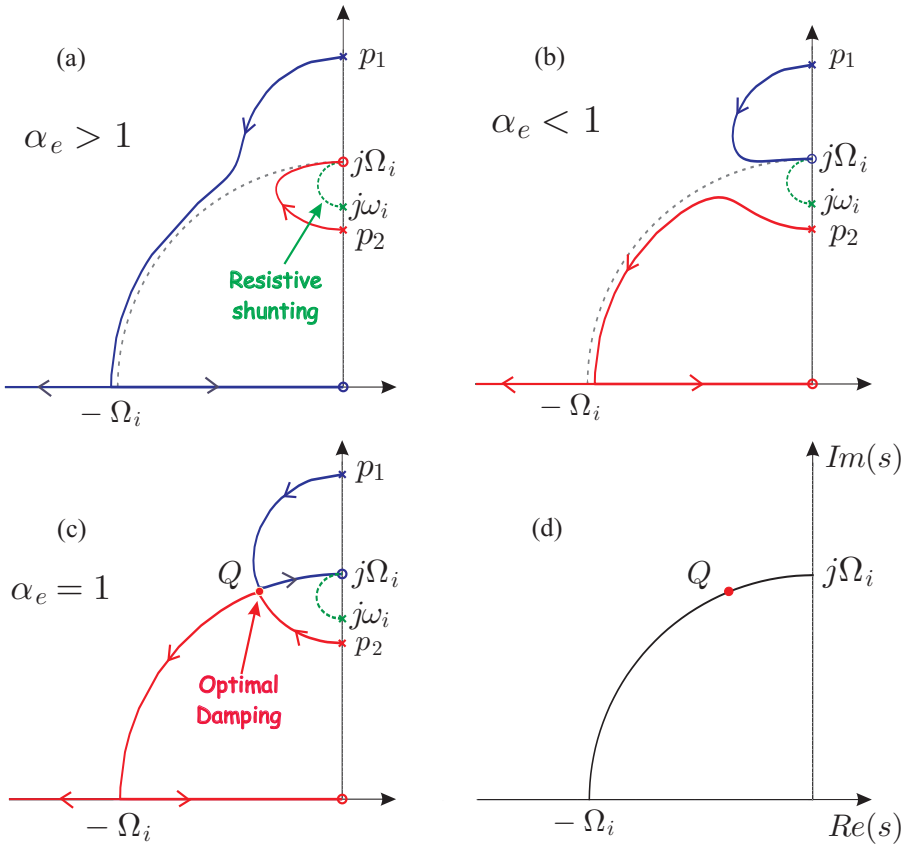

Fig. 8. Root locus plot for inductive shunting (only the upper half is shown). The optimum damping at Q is achieved for $\alpha_e = 1$ and $\xi_e = K_i^2$; the maximum modal damping is $\xi_i \simeq K_i/2$.

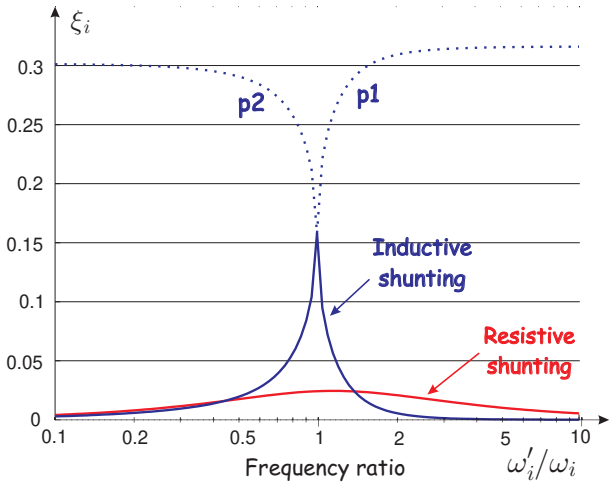

Fig. 9. Evolution of the damping ratio of the inductive and resistive shunting with the de-tuning of the structural mode. ω_i is the natural frequency for which the shunt has been optimized, ω_i' is the actual value ($k = 0.5$, $\nu_i = 0.3$).

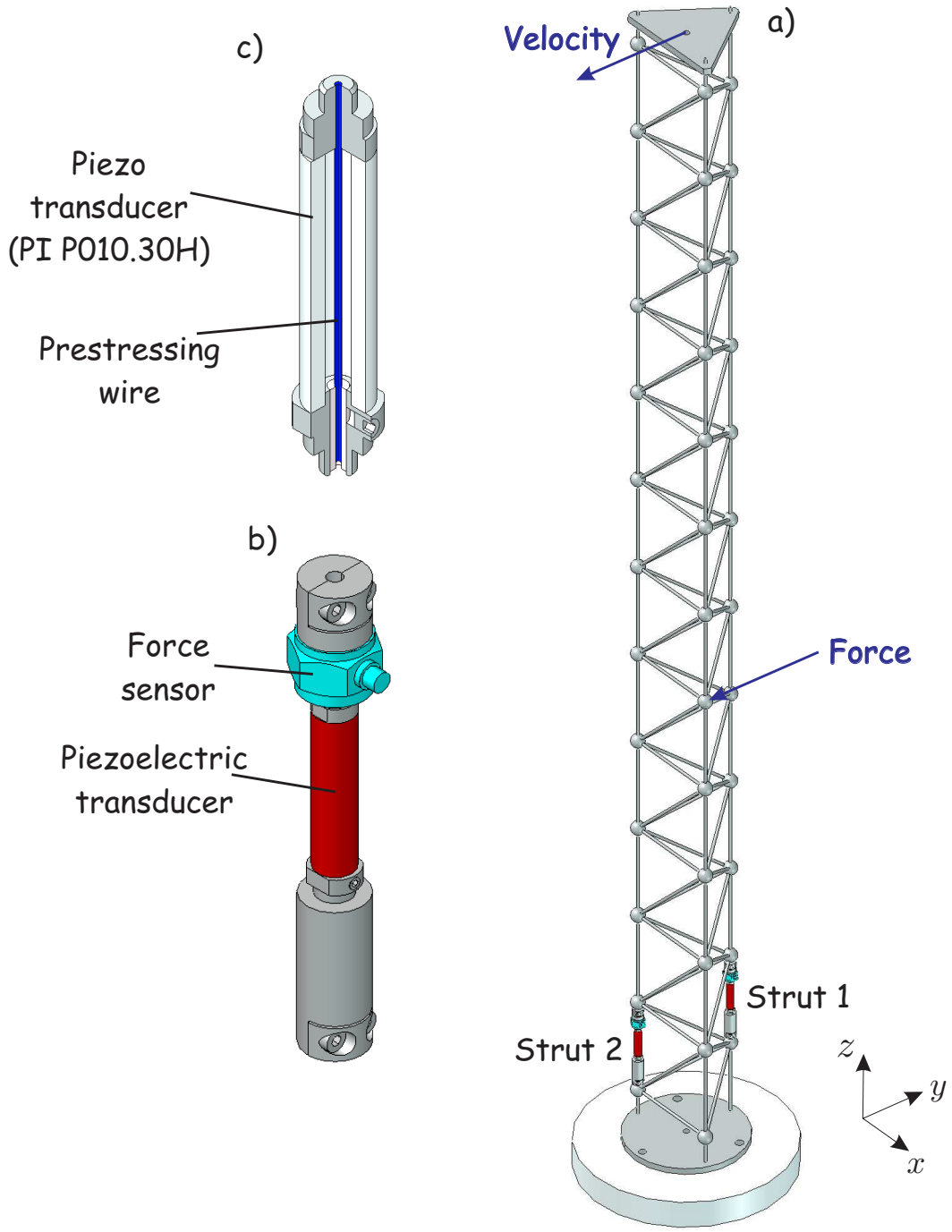

Fig. 10. (a) Truss structure considered in the numerical example. (b) Detail of an active strut consisting of a linear piezoelectric transducer and a force sensor. (c) Exploded view of the piezoelectric transducer showing the prestressing wire.

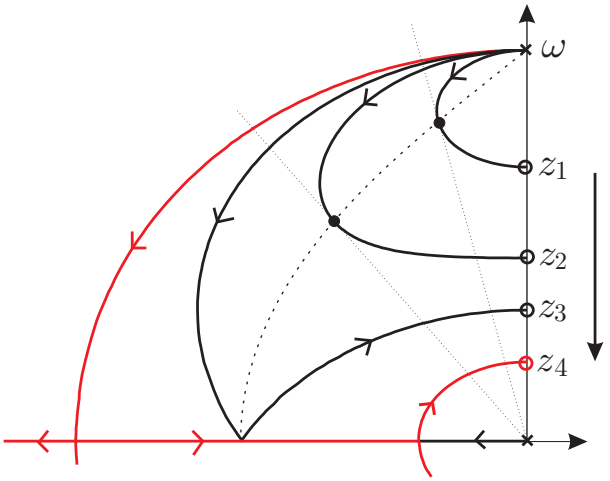

Fig. 11. Evolution of the root locus of the closed-loop poles of the IFF when the open-loop zeros migrate to the origin. The locus exactly touches the real axis for $z_3 = \omega/3$. The dotted line corresponds to the maximum damping given by (24).

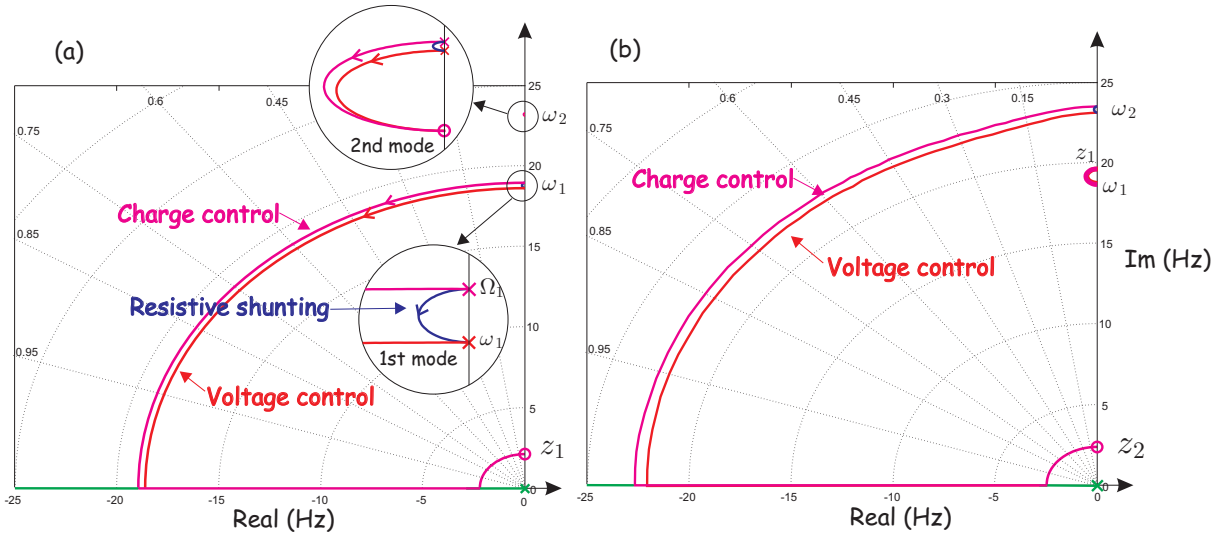

Fig. 12. Root locus of the IFF with voltage control, charge control and resistive shunting. (a) Strut 1 (b) Strut 2. The frequencies are given in *Hz*.

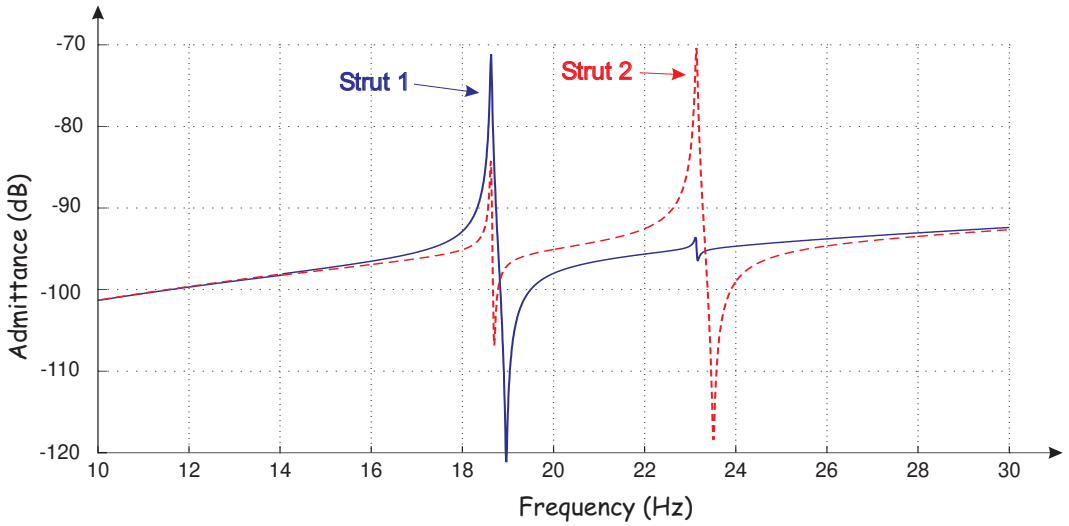

Fig. 13. Predicted admittance of strut 1 and strut 2.

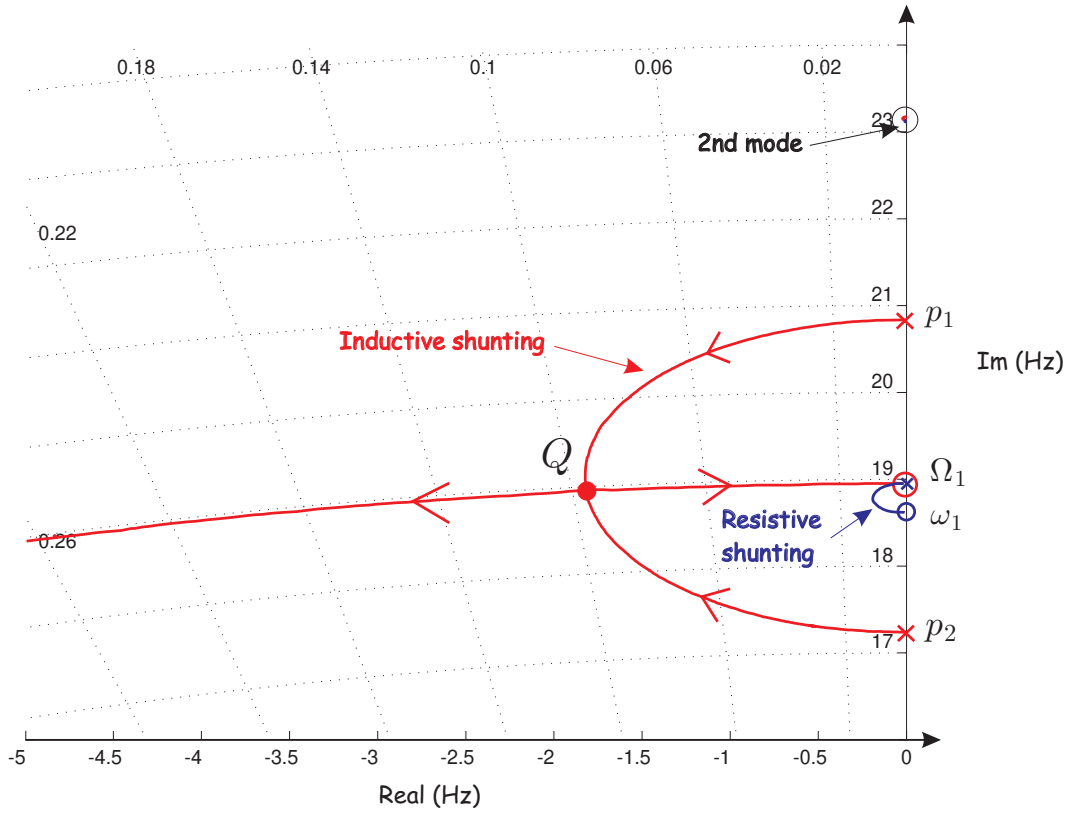

Fig. 14. Inductive shunting of strut 1, detail of the root locus in the vicinity of mode 1 for perfect tuning of the electrical tuning of the electrical circuit.

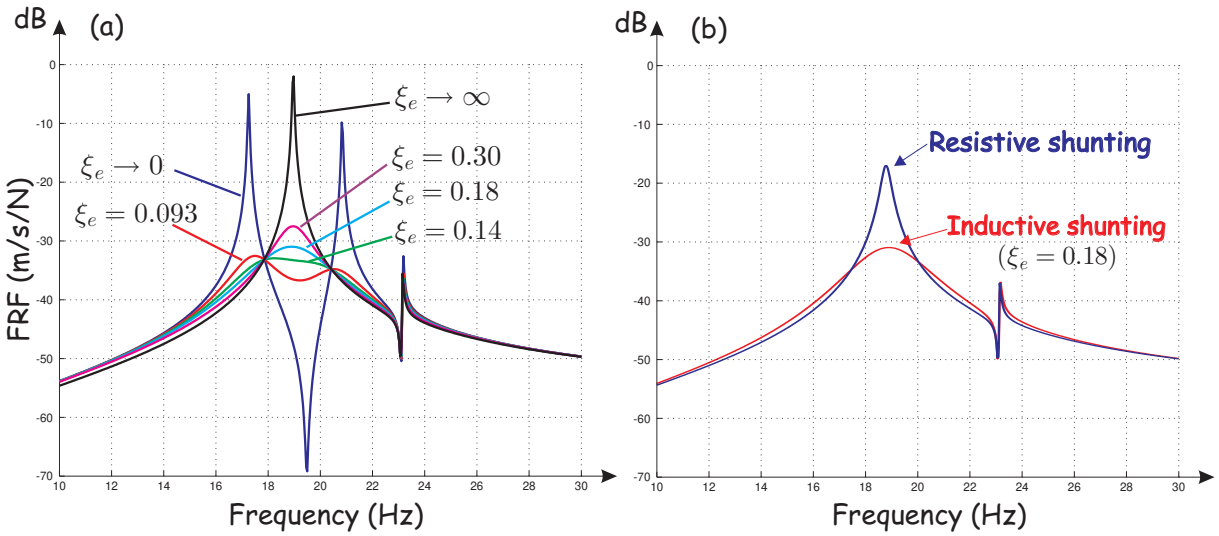

Fig. 15. FRF between a lateral force applied along the truss and the velocity at the top (see Fig.10). (a) Inductive shunting with optimal frequency tuning: evolution of the FRF with the electrical damping. (b) Comparison of resistive and inductive shunting (both at optimum value).

Table 1
Open-loop poles and zeros and maximum achievable modal damping in the root locus of Fig.5. The inductive shunting is added for comparison.

Control	Open-loop poles	Open-loop zeros	Max. Damping ξ_i
IFF (Voltage control)	$\pm j\omega_i$ *(short-circuit)*	$\pm j z_i \simeq \pm j\omega_i\sqrt{1-\nu_i}$	$\frac{\nu_i}{4(1-\nu_i)}$
IFF (Charge control)	$\pm j\Omega_i \simeq \pm j\omega_i\sqrt{1+\frac{k^2\nu_i}{1-k^2}}$	$\pm j z_i$ *(transducer removed)*	$\frac{\nu_i}{4(1-\nu_i)(1-k^2)}$
Resistive shunting	$\pm j\Omega_i$ *(open electrodes)*	$\pm j\omega_i$	$\frac{k^2\nu_i}{4(1-k^2)}$
Inductive shunting	p_1, p_2	0 , $\pm j\Omega_i$	$\frac{1}{2}\sqrt{\frac{k^2\nu_i}{1-k^2}}$

Table 2
Natural frequencies (in Hz) with short-circuited electrodes and fractions of modal strain energies for strut 1 and 2.

mode	$\omega_i/2\pi$	ν_i (%)	
		strut 1	strut 2
1	18.63	9.65	2.07
2	23.14	0.17	8.60
3	102.98	1.32	0.17
4	109.51	1.05	4.84
5	124.32	0.13	2.47
6	228.15	0.50	2.65

Table 3
Predicted Ω_i (in Hz), K_i, z_i (in Hz) (**1**) approximate formulae and (**2**) specific FE models.

	mode	$\Omega_i/2\pi$		K_i (%)		z_i (%)	
		(1)	**(2)**	**(1)**	**(2)**	**(1)**	**(2)**
strut 1	1	19.13	18.96	22.69	18.61	17.71	2.14
	2	23.15	23.14	3.09	2.58	23.12	23.07
strut 2	1	18.74	18.69	10.73	8.25	18.44	19.57
	2	23.69	23.51	21.48	17.67	22.12	2.40

Table 4
Predicted maximum modal damping ξ_i (in %) for the IFF and resistive shunting. (**1**) approximate formulae, (**2**) specific FE models, (**3**) full MATLAB model.

	mode	IFF (Voltage)			IFF (Charge)			Resistive shunting		
		(1)	**(2)**	**(3)**	**(1)**	**(2)**	**(3)**	**(1)**	**(2)**	**(3)**
strut 1	1	2.60	critical	critical	4.01	critical	critical	1.34	0.90	0.89
	2	0.04	0.15	0.15	0.07	0.17	0.17	0.024	0.017	0.017
strut 2	1	0.53	2.40	2.86	0.82	2.07	2.60	0.29	0.17	0.17
	2	2.30	critical	critical	3.55	critical	critical	1.20	0.80	0.80

Table 5
Inductive shunting, optimum electrical parameters ($\omega_e/2\pi$ in Hz) and predicted maximum modal damping. (**1**) approximate formulae, (**2**) specific FE models, (**3**) full MATLAB model.

		$\omega_e/2\pi$			ξ_e (%)			ξ_i (%)		
	mode	**(1)**	**(2)**	**(3)**	**(1)**	**(2)**	**(3)**	**(1)**	**(2)**	**(3)**
strut 1	1	19.64	19.30	19.78	22.69	18.61	18.19	11.65	9.47	9.45
strut 2	2	24.26	23.88	24.56	21.48	17.67	17.44	11.00	8.98	8.91